RAPID POST-EARTHQUAKE SAFETY EVALUATION OF BRIDGES

Roy A. Imbsen[1], P.E., D.Engr.
Shahriar Vahdani[2], P.E., Ph.D.
Jinquan Zhong[1], P.E., Ph.D.

[1]SC Solutions, Inc. Sunnyvale, CA
[2]Applied Geodynamics, Inc., El Cerrito, CA

Abstract

A new procedure for rapid post-earthquake safety evaluation of bridges is being developed, using existing strong motion records, PGA data immediately available following an earthquake, and fragility databases, to assist responsible parties in making timely, informed decisions regarding post-earthquake bridge closures. The New Carquinez Bridge was selected to demonstrate the procedure. This paper provides a procedure overview and its application to safety evaluation of a bridge following an earthquake event, and the development to date of this process, including earthquake scenario selection and generation of ground motions for nonlinear time history analyses of the bridge to establish component fragility data.

Introduction

This study, entitled *Rapid Post-Earthquake Safety Evaluation of the New Carquinez Bridge Using Fragility Curves and Recorded Strong-Motion Data* is part of the Data Interpretation Project of the California Strong Motion Instrumentation Program (CSMIP) in the Department of Conservation (DOC) California Geological Survey. The purpose of this project is to accelerate the application of the strong-motion data in reducing risk due to the strong earthquake shaking which occurs in California.

Figure 1. Aerial View of the New Carquinez Bridge.

The application of the procedure undertaken in this study is to provide for the selected New Carquinez Bridge, as shown in Figure 1, the ability to assess the damage immediately following an earthquake using the ground motion parameters of the earthquake event and fragility curves developed for the bridge so that a decision can be made on the continued use or closure of the bridge.

Overview of the Safety Evaluation Procedure

SC Solutions was tasked to develop a system to improve the current Caltrans rapid post-earthquake decision making process for critical bridges. Immediately after any earthquake, Caltrans has to make decisions about the post-earthquake conditions of bridges. The decision making process will be based on the earthquake intensity, location of a bridge, instrument data, the understanding of the performance of the bridge in the subject earthquake, and other factors related to risk and consequences. Most of the critical bridges that are in high seismic zones are instrumented. These instrument data are monitored in real time and can be used for this decision making process. The foundation or free field ground motions near the bridge and some of the structural performance can be obtained immediately after an earthquake. However, this limited instrument data doesn't provide adequate information about the conditions of all critical components of bridges immediately after an event. Therefore, additional understanding of the bridge performance and fragility functions should be developed for each of these critical bridges to assist the post-earthquake decision making process.

To develop fragility functions, first a set of pre-earthquake scenario events must be selected based on the location of the bridge and the active faults in the vicinity of the bridge site. For this task SC Solution proposed to use the New Carquinez Bridge for the case study. After selecting a set of scenario earthquakes for the New Carquinez Bridge, the existing SC Solutions bridge model could be used to simulate the effects of these ground motions to understand the performance of each critical component in the bridge. After conducting these pre-earthquake seismic analyses, a relationship can be developed between the earthquake intensity parameter (e.g. PGA and spectral acceleration) and the primary response parameter of a critical component. As one example, the primary response parameter can be a drift for a critical tower. Based on the primary response parameter value a damage index (or damage potential) can be developed for each critical component. This damage potential can be related to the seismic intensity parameter as a fragility function for each critical component.

Pre-Event Data Processing

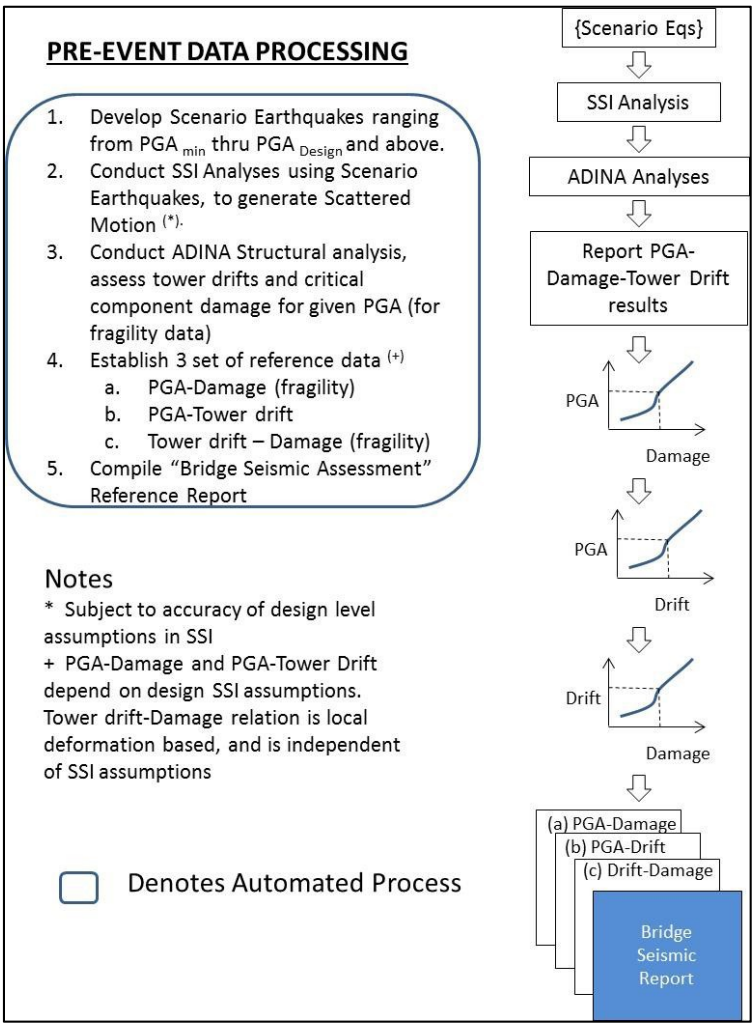

Figure 2. Pre-Event Data Processing.

As shown in Figure 2, prior to an event, several automated procedures will be completed and compiled in a "Bridge Seismic Assessment" report, as a reference document for Caltrans decision making, after an event. The steps include the following:

1. A series of scenario ground motions will be generated based on different magnitude earthquakes on regional faults. These motions will range from low fault activity and spectral acceleration, through Design Spectra, and spectral acceleration values both less than and greater than design levels prescribed for the site.

2. Using the available site specific ground motion, generation tools and design spectra, the SSI analytical model customized for the Carquinez site will be used to bring the scenario earthquakes to the site and to generate scattered motions.

3. The existing Finite Element model of the New Carquinez Bridge, developed by SC Solutions, will be used in the demand analyses under the scenario ground motions. Damage status of critical components of the bridge will be related to spectral acceleration (i.e. fragility data). For each critical component, a primary response parameter will be identified. For example for critical tower member and connections, "Tower Drift" will be the governing primary response parameter. The proposed approach and scope-of-work is based on the use of Tower 3 Drift as the primary response parameter to reflect the damage state of Critical Tower Components, as an example of the process. This methodology can be applied to different primary response parameters to reflect damage status of other critical components. For example foundation movements can reflect pile damage; superstructure movement can reflect damage to critical superstructure components and expansion joints; or cable movements which can reflect condition of cable anchorage.

4. Governing Tower drifts as the primary response parameters will also be documented vs. spectral acceleration, and finally series of relations between Tower Drift and Damage state of the critical tower components will be generated.

5. Based on the analyses, the following response parameters will be related to the scenario earthquake intensity, fault, and distance to site:

   a. Spectral acceleration versus Damage index of critical components (Fragility),

   b. Spectral acceleration versus Tower Drift,

   c. Tower Drift versus Damage index of critical components,

Description of the New Carquinez Bridge and Local Seismic Design Hazard

Description of the New Carquinez Bridge

The New Carquinez Bridge spans the Carquinez Strait with a 2,388 ft. main span bounded by a south span (towards Oakland) of 482 ft. and a north span (towards Sacramento) of 594 ft. as shown in Figure 3. The principal components of this suspension bridge include reinforced concrete towers supported on large-diameter concrete pile foundations, parallel-wire cables, gravity anchorages, and a closed orthotropic steel box deck system. The main concrete towers are approximately 400 ft. tall, and are tied together with a strut below the deck and an upper strut between the cable saddles as shown in the Typical Section view included in Figure 3. The lower strut supports the deck vertically using two rocker links and transversely through a shear key.

The bridge site, located approximately twenty miles northeast of San Francisco, is located in an active seismic zone. Seismic hazard assessments have shown that the site could be subject to strong ground motions originating on the San Andreas Fault, the Hayward Fault, Concord-Green Valley, Napa Valley, and the Franklin Fault. However, studies have shown that the Hayward fault, Concord-Green Valley fault system, and the Napa Valley seismic zones are the dominant sources of seismic hazard for the bridge's frequency range.

The seismic design of the New Carquinez Bridge considers both the Safety Evaluation Earthquake (SEE) and the lower level Functional Evaluation Earthquake (FEE). Caltrans performance requirements for these events are higher than the minimum level required for all transportation structures but below that required for an Important Bridge. As much as possible, the Important Bridge criteria are to be met for the Safety Evaluation Earthquake (SEE) corresponding to a maximum credible event which has a mean return period in the range of about 1,000 to 2,000 years. In this earthquake, the bridge can be subject to primarily "minor" damage with some "repairable" damage to piles, pile caps and anchorage blocks and still remain open.

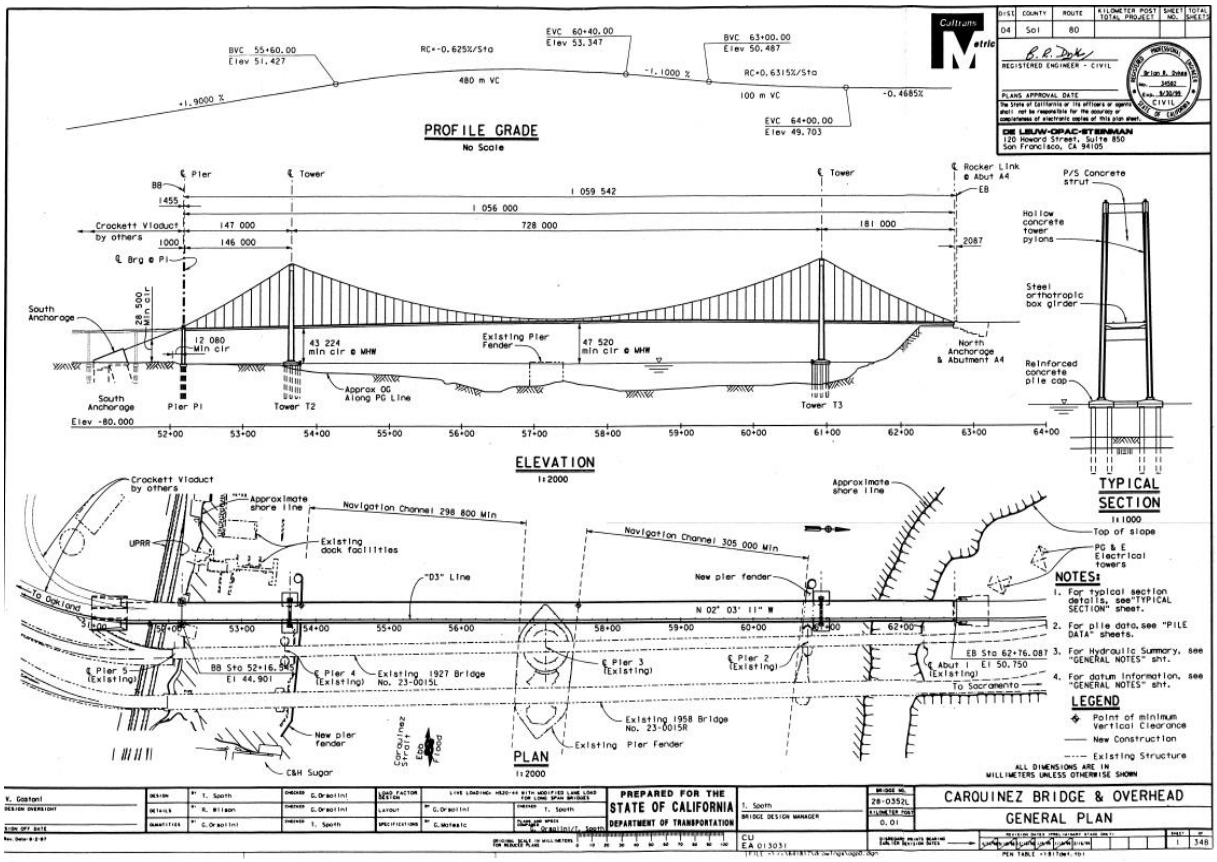

Figure 3. General Plan of the New Carquinez Bridge.

New Carquinez Bridge Local Seismic Design Hazard

For the New Carquinez Bridge, the resulting design response spectra for the Franklin, Hayward, and San Andreas events the values of peak design rock accelerations are taken from the original bridge design report (DLOS, 1999, Third Carquinez Strait Bridge, Seismic Report), and are as follows:

Source/MCE/Distance	Peak Rock Acceleration (g's) Horizontal PGA	Vertical PGA
San Andreas, M_w 8, R=41 km	0.26	0.19
Hayward, M_w 7¼, R=13 km	0.55	0.47
Franklin, M_w 6½, R=1 km	1.00	0.96

Determination of Dynamic Characteristics for the Conditional Mean Spectra (CMS).

Using the results from the dynamic response analysis conducted on the New Carquinez Bridge by SC Solutions for the design, the dynamic characteristics were readily available to determine the periods, mode shapes, and participation factors that were the major contributors to the dynamic response of Tower 3 in the longitudinal direction for Tower 3. Although there are other modes with larger participation factors in the longitudinal direction, their contribution to the longitudinal participation is very small. As shown in Table 1, Modes 11, 12, 13 and 19 show the largest longitudinal mass participation. Therefore it can be concluded that the modes having periods ranging from 2.18 to 2.64 seconds were the primary contributors to the longitudinal response of Tower 3. A target period of 2.4 seconds, within the range, was selected as the target period for the Conditional Mean Spectra (CMS). Conditional Mean Spectra at the period of the tower were developed using the Baker (2011) and Jayaram and Baker (2008) procedure as described below. We judge that the CMS would provide more realistic ground motions than the deterministic 84th percentile ground motions from the ground motion prediction equations (GMPEs) as described in more detail below. Shown in Figure 4 are three views of the displaced shape for Mode 11. Figure 5 shows an enlarged isometric view of Mode 11.

Table 1 Dynamic Response-Modes, Periods and Participation

	Period	mass			accumulated mass		
Mode #	(sec)	MASS(X)	MASS(Y)	MASS(Z)	MASS(X)	MASS(Y)	MASS(Z)
2	6.66	1%	11%	0%	1%	11%	0%
5	4.15	0%	4%	2%	1%	15%	2%
11	2.65	10%	9%	1%	11%	24%	4%
12	2.64	9%	0%	1%	21%	24%	5%
13	2.54	6%	0%	0%	27%	24%	5%
19	2.18	8%	9%	0%	35%	34%	5%
21	2.12	0%	8%	0%	35%	42%	5%
67	0.76	13%	24%	3%	48%	66%	8%
88	0.62	17%	1%	1%	65%	67%	9%

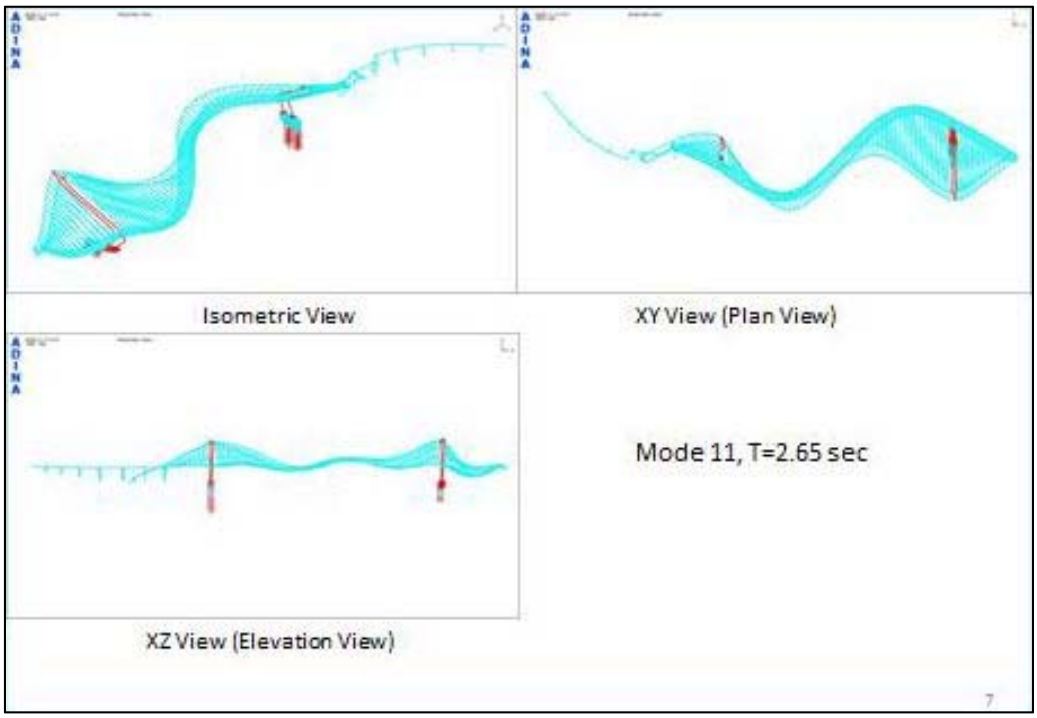

Figure 4. Various Views Showing the Displaced Shape for Mode 11.

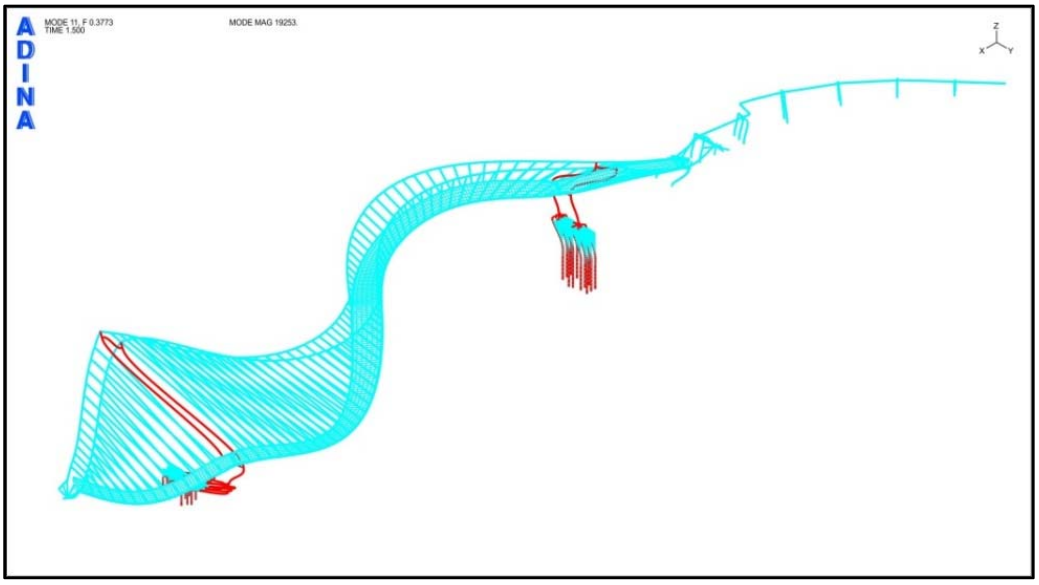

Figure 5. Enlarged Isometric View of Mode 11.

Development of the Scenario Earthquakes

The development of 26 sets of ground motions (each set with two horizontal components and one vertical component) used for time history analysis of the New Carquinez Bridge follows standard practices in determining moment magnitude (Mw) and site-to-source distance (R) of earthquake scenarios and site conditions, computing horizontal and vertical design spectra, selecting seed motions, and spectrally matching selected seed motions. This section presents the details of the procedures used in the ground motion development for 16 different scenario earthquakes (SCS, 2015), i.e., the first 26 scenario earthquakes listed in Table 2 below. Among these 26 scenario earthquakes, 15 of them are designated to have velocity pulses in order to consider directivity effects from near-fault motions. The percentage of scenario earthquakes with velocity pulses is about 60%, consistent with the fraction of ground motions with velocity pulses used for nonlinear time-history analysis in current practice. Figure 6 below shows the significant earthquakes which have happened between 1970 and 2003 and the faults around the bridge site.

Table 2. Selected Scenario Earthquakes for the Pre-Earthquake Analysis

Scenario	Mw	R (km)	Probability Level	Directivity	Pulse Period Tp (Sec.)	Set of Time Histories	Causative Fault
1-3	7.3	13	84th percentile CMS@2.4 sec	Yes	+/- 4.7	3	Hayward+ Rodgers Creek
4	7.3	13	84th percentile CMS@2.4 sec	No	-	1	Hayward+ Rodgers Creek
5	7.3	13	50th percentile	No	-	1	Hayward+ Rodgers Creek
6-8	6.8	13	84th percentile CMS@2.4 sec	Yes	+/- 3.7	3	Hayward/ Green Valley
9	6.8	13	84th CMS@2.4 sec	No	-	1	Hayward/ Green Valley
10	6.8	13	50th percentile	No	-	1	Hayward/ Green Valley
11	6.8	28	84th percentile CMS@2.4 sec	No	-	1	Calaveras
12-14	6.3	13	84th percentile CMS@2.4 sec	Yes	+/- 2.9	3	Hayward
15	6.3	13	84th percentile CMS@2.4 sec	No	-	1	Hayward
16	6.3	13	50th percentile	No	-	1	Hayward
17	6.3	20	50th percentile	No	-	1	Hayward/ Green Valley
18-20	5.8	13	84th percentile CMS@2.4 sec	Yes	+/-2.2	3	Hayward
21-23	6.5	1	0.5(50th+84th)	No	+/-2.3	3	Franklin
24	7.9	42	84th percentile CMS@2.4 sec	No	-	1	San Andreas
25	7.9	42	50th percentile	No	-	1	San Andreas
26	6.5	12	50th percentile	No	-	1	Caltrans Min.
27	6.0	20	-	-	-	1	2014 Napa Event

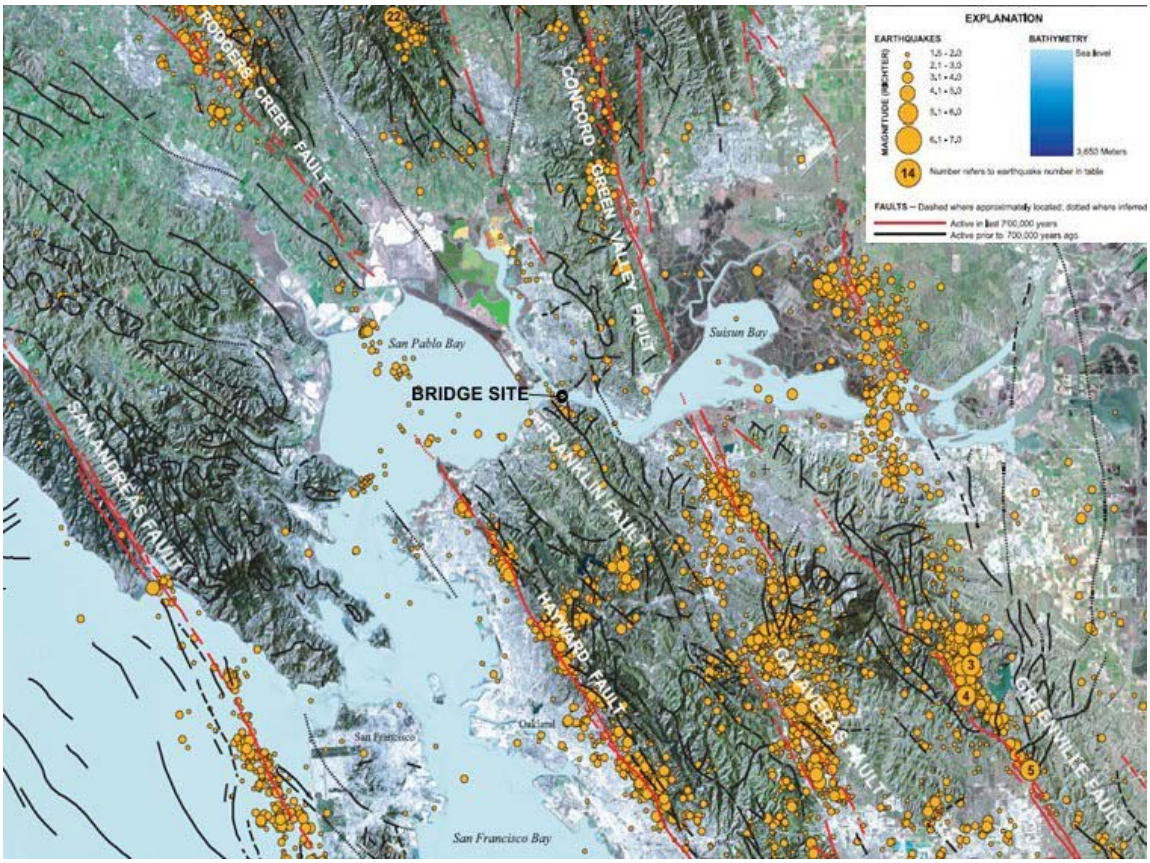

Figure 6. Earthquakes Occurring Between 1970 & 2003 and Faults around the New Carquinez Bridge (after Sleeter et al., 2004)

Horizontal and Vertical Design Spectra

Based on the 26 scenario earthquakes listed in Table 2, horizontal and vertical design spectra were developed at the control point (EMI, 2014) at CGS Array #2 (located to the west of the south anchorage of the bridge), as shown in Figure 7, with a Vs30 value estimated at 305 m/s per EMI (2014) and the original bridge design report (DLOS, 1999). The geometric mean (geomean) of the horizontal design spectra was computed by using four equally-weighted ground motion prediction equations (GMPEs), i.e., ASK14 (Abrahamson et al., 2014), BSSA14 (Boore et al., 2014), CB14 (Campbell and Bozorgnia, 2014), and CY14 (Chiou and Young, 2014), from the NGA-West2 database (Ancheta et al., 2014).

For Scenarios 1-3, 6-8, 12-14, and 18-20, directivity effects (Somerville et al., 1997, Abrahamson, 2000) were incorporated into the developed geomean of the design spectra to develop the fault average (FA) design spectrum, which was further resolved into fault normal (FN) and fault parallel (FP) design spectra. To arrive at a more realistic design spectrum, a conditional mean spectra (Baker, 2011) for FN and FP design spectra were developed, for each

of these scenarios at 2.4 seconds, the period most significantly contributing to the longitudinal response of Tower 3 of the New Carquinez Bridge.

For Scenarios 21-23 (the original design event), the average of the 50th and 84th percentiles of geomean spectra computed from NGA-West2 GMPEs was used as the FA design spectrum to avoid undue conservatism due to the high uncertainty regarding the existence, location, and activity of the Franklin fault. The FA spectrum was further resolved into FN and FP design spectra using the factors determined from DLOS (1999). To determine the FN design spectrum, the ratios between FN and FP design spectra presented in DLOS (1999) were calculated and applied to the FA design spectrum. The FP design spectrum was taken to be the same as the FA design spectrum.

The geomean spectra (at the 50th percentile) were used as the horizontal design spectra for Scenarios 10, 16, 17, 25, and 26. CMS was developed for Scenarios 4, 9, 11, 15, and 24 based on the geomean of horizontal spectra (at the 84th percentile) at 2.4 seconds.

The developed horizontal design spectra, including geomean, CMS, FN and FP design spectra, for all 26 scenarios are presented in Figure 8. From this figure it can be seen that the FN and FP design spectra for Scenarios 1-3 are larger than the original design event at 2.4 seconds while the horizontal spectra for other scenarios are lower than the original design event at 2.4 seconds. Once all horizontal design spectra are determined, the V/H ratios developed by Gülerce and Abrahamson (2011) were then multiplied with horizontal (geomean, CMS, or FA design spectrum as appropriate) design spectra for vertical spectra. The computed vertical design spectra for all 26 scenarios are presented in Figure 9. Vertical design spectra for all 26 scenarios

Figure 7. Plan View of CGS Array#2 at the South End of the New Carquinez Bridge Located at Latitude and Longitude of (38.0545, -122.2264)

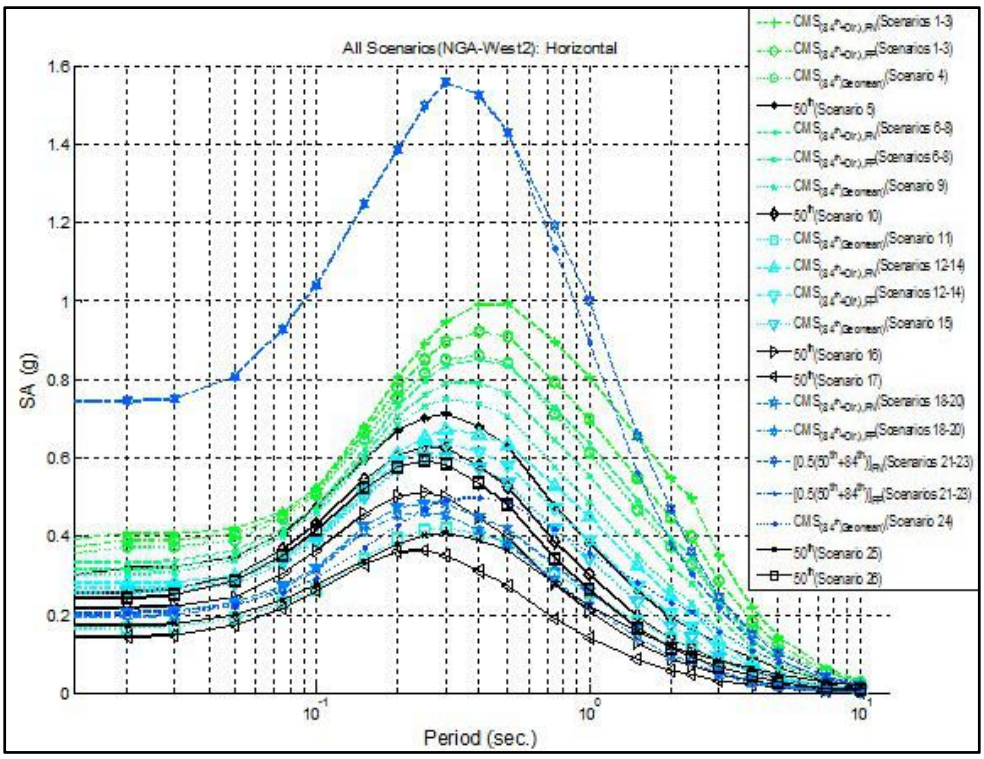

Figure 8. Horizontal design spectra for all 26 scenarios.

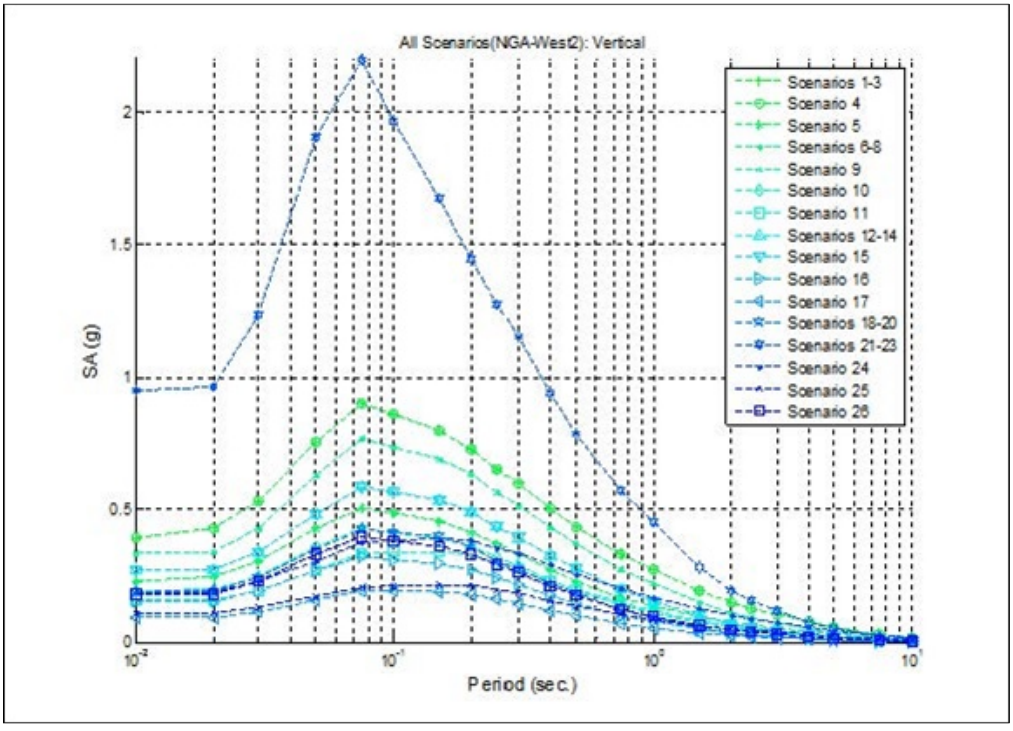

Figure 9. Vertical design spectra for all 26 scenarios.

Selection of Seed Motions

The NGA-West2 database provides 19,880 sets of recorded motions with three-component time histories available in digital formats. In these available recorded motions, the magnitudes vary from 2.9 to 7.9, the site-to-source distances vary from 0.05 to 1,156.9 km, Vs30 values vary from 89 m/s to 2,100 m/s, and periods of velocity pulse (Tp) vary from 0.322 seconds to 13.120 seconds. In particular, there are 142 sets of recorded motions with velocity pulse in the NGA-West2 database.

The six factors discussed below (listed in priority order) were considered in selecting 26 sets of seed motions (each with two horizontal components and one vertical component) suitable for further spectral matching:

1. Tp of the horizontal component of seed motion is similar to the target Tp computed to be consistent with magnitude and site-to-source distance (Shahi and Baker, 2011). The target Tp values considered in seed motion selection are listed in Table 3 below:

Table 3. Period of velocity pulses for 15 scenarios with directivity effects

Scenarios	Mw	R (km)	Tp (sec.)
1-3	7.3	13.0	4.7
6-8	6.8	13.0	3.7
12-14	6.3	13.0	2.9
18-20	5.8	13.0	2.2
21-23	6.5	1.0	2.3

2. Moment magnitude of seed motion is close to the magnitude of scenarios listed in Table 2;
3. Site-to-source distance of seed motion is close to the magnitude of scenarios listed in Table 2;
4. Seed motion recorded at site condition with Vs30 values is close to the target 305 m/s;
5. The spectral shape of each component of a seed motion is similar to the target design spectrum (horizontal or vertical as appropriate); and
6. Waveforms of each component of a seed motion are similar to the target, with distinguishable arrivals of P- and S-waves.

Table 4 below lists the metadata for the seed motions selected from the NGA-West2 database for further spectral matching in terms of RSN number in the NGA-West2 database, earthquake event, year, record station, Mw, R, Vs30, and Tp values. Note that the source-to-site distances for 12 of the selected seed motions (for Scenarios 1-3, 6-8, 12-14, and 18-20) are all smaller than 13km. The selected seed motions represent the balance among all six factors considered with the highest priority given to Tp values close (+/– 1 second) to the values listed in Table 3, as opposed to one single factor of source-to-site distance.

Table 4. Metadata for 26 Sets of Seed Motions Selected from the NGA-West2 Database

Scenario	RSNno	Earthquake Event	Year	Record Station	Mw	R (km)	Vs30 (m/s)	Tp (sec.)
1-3	1176	Kocaeli Turkey	1999	Yarimca	7.51	1.38	297.00	4.95
	292	Irpinia Italy-01	1980	Sturno (STN)	6.90	6.78	382.00	3.28
	1244	Chi-Chi Taiwan	1999	CHY101	7.62	9.94	258.89	5.31
4	864	Landers	1992	Joshua Tree	7.28	11.03	379.32	-
5	5831	El Mayor-Cucapah Mexico	2010	EJIDO SALTILLO	7.20	14.80	242.05	
6-8	1045	Northridge-01	1994	Newhall - W Pico Canyon Rd.	6.69	2.11	285.93	2.98
	1114	Kobe Japan	1995	Port Island (0 m)	6.90	3.31	198.00	2.83
	161	Imperial Valley-06	1979	Brawley Airport	6.53	8.54	208.71	4.42
9	4847	Chuetsu-oki Japan	2007	Joetsu Kakizakiku Kakizaki	6.80	9.43	383.43	-
10	6961	Darfield New Zealand	2010	RKAC	7.00	13.37	295.74	-
11	6923	Darfield New Zealand	2010	Kaiapoi North School	7.00	30.53	255.00	-
12-14	292	Irpinia Italy-01	1980	Sturno (STN)	6.90	6.78	382.00	3.28
	8123	Christchurch New Zealand	2011	Christchurch Resthaven	6.20	5.11	141.00	1.55
	1045	Northridge-01	1994	Newhall - W Pico Canyon Rd.	6.69	2.11	285.93	2.98
15	313	Corinth Greece	1981	Corinth	6.60	10.27	361.40	-
16	8099	Christchurch New Zealand	2011	Kaiapoi North School	6.20	17.86	255.00	-
17	4078	Parkfield-02 CA	2004	Coalinga - Fire Station 39	6.00	22.45	333.61	-
18-20	569	San Salvador	1986	National Geografical Inst	5.80	3.71	455.93	1.13
	147	Coyote Lake	1979	Gilroy Array #2	5.74	8.47	270.84	1.46
	149	Coyote Lake	1979	Gilroy Array #4	5.74	4.79	221.78	1.35
21-23	1120	Kobe Japan	1995	Takatori	6.90	1.46	256.00	2.49
	159	Imperial Valley-06	1979	Agrarias	6.53	0.00	242.05	2.28
	1054	Northridge-01	1994	Pardee - SCE	6.69	5.54	325.67	2.05
24	1236	Chi-Chi Taiwan	1999	CHY088	7.62	37.48	318.52	-
25	2111	Denali Alaska	2002	R109 (temp)	7.90	42.99	341.56	-
26	313	Corinth Greece	1981	Corinth	6.60	10.27	361.40	-

Spectral Matching of Selected Seed Motions

The selected seed motions in Table 4 were spectrally matched to a 5%-damped target spectra for the frequency range of interest, i.e., between 0.2 Hz and 2.0 Hz. Although we focused on this frequency range during spectral matching, additional attempts were taken to match frequencies beyond this range, usually between 0.2 Hz and 100 Hz, without significantly altering the waveform character of the seed motions.

Before spectral matching, a linear scaling factor was applied to each seed motion component such that each seed motion component had the same spectral ordinate as that of the target spectrum at 100 Hz. The scaled seed motion component was then spectrally matched to the 5%-damped target design spectrum using RSPMatch09 (Atik and Abrahamson, 2009).

To limit the number of frequencies used to compute the response spectrum, the requirements of ASCE 4-98 and Section 2.4(b) of ASCE43-05 on the number of and the spacing of frequencies were followed:

1. The frequencies shall be calculated such that each frequency is within 10% of the previous frequency (or alternatively use Table 2.3-2 of ACSE 4-98); and
2. Spectral accelerations shall be computed for at least 100 points per frequency decade and uniformly distributed on a $\log_{10}$ scale between 0.1 to 50 Hz.

To meet both requirements, 315 frequencies were populated over the frequency range of 0.1 Hz to 100 Hz for spectral matching. The tolerance between the 5%-damped response spectrum of each SMM component and the target design spectrum was set at +/-5% of the target spectrum.

Rotation of Horizontal Components into Longitudinal and Transverse Bridge Directions

After the spectral matching, the FN and FP components need to be rotated into the longitudinal and transverse directions of the New Carquinez Bridge for fragility analysis. The angles used to rotate the FN and FP components into the longitudinal and transverse directions of the bridge are measured from the projected fault line to the longitudinal axis of the bridge. The rotation angles from each fault line to the longitudinal axis of the bridge are listed in Table 5 below. For all other scenarios, the H1 and H2 components can be applied directly into to the longitudinal and transverse axes of the New Carquinez Bridge.

Table 5. Angles Measured from Projected Fault Line to the Longitudinal Axis of the Bridge

Scenarios	Fault Name	θ (deg., measured clock wise from fault line to the longitudinal axis)
1-3	Hayward/Rodgers Creek	20.3
6-8	Hayward/Green Valley	2.3
12-14	Hayward	20.3
18-20	Hayward	20.3
21-23	Franklin	18.0

Future Development Tasks: Time History Analyses & Fragility Database

Time History Analysis

The SC Solutions Finite Element (FE) models of the New Carquinez Bridge, as shown in Figure 10, has been verified and correlated with both physical testing and with models developed by others. Shown in Figure 10 is the ADINA model for both a simple model and a more complex finite element model. The bridge is fully instrumented with sensors placed on the bridge as shown in Figure 11 and Figure 12. At this stage in the project several families of scenario ground motions have been generated as described above. These motions are being applied to the bridge to establish critical component fragilities and corresponding tower drift data, to be included in the "Bridge Seismic Assessment" report. This process of using the available ADINA FE model for all earthquake scenarios, and to extract fragility and drift information will be developed and automated so that it can be repeated efficiently to accommodate any adjustments to design or earthquake intensities for future projects or post-earthquake investigations.

Fragility Database

A Fragility Database will be generated using the results from the time history analyses of the developed time history ground motions. The FE model is used to assess the response of critical bridge components with their appropriate CMS as described above, and relate their response to the event strength (PGA). In addition, for each event, tower response parameters that include drift, displacements, bending moments and shear forces, concrete and steel strains, and curvatures will also be processed and reported to correlate with the observed damage states and response parameters obtained in the research conducted by Vosooghi and Saiidi (2010). In their work they obtained data from 32 bridge column models, most of which were tested on a shake table, to develop fragility curves for the seismic response of reinforced concrete bridge columns. Photographs of the physical damage imparted to the test columns were taken during the testing to correlate with the analytical models and the measured concrete and steel strains in the test columns.

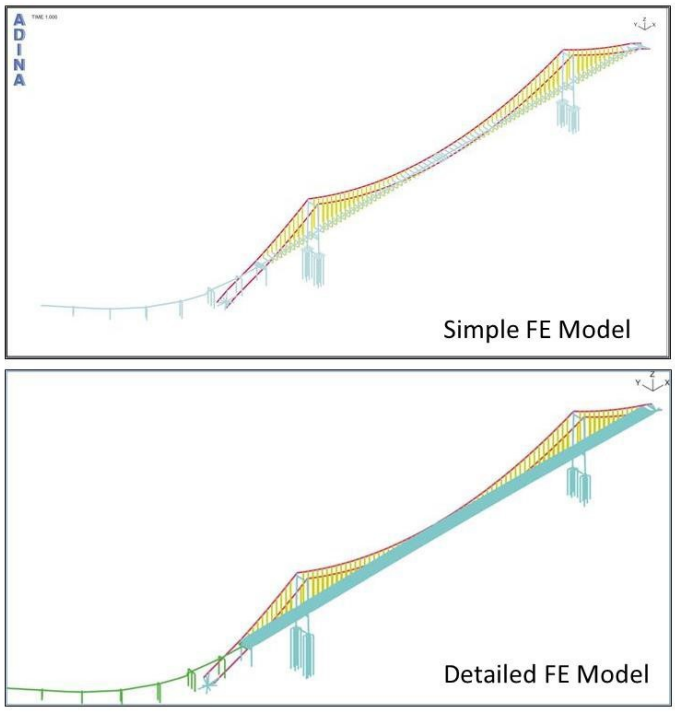

Figure 10. SC Solutions' Finite Element Models for the New Carquinez Bridge.

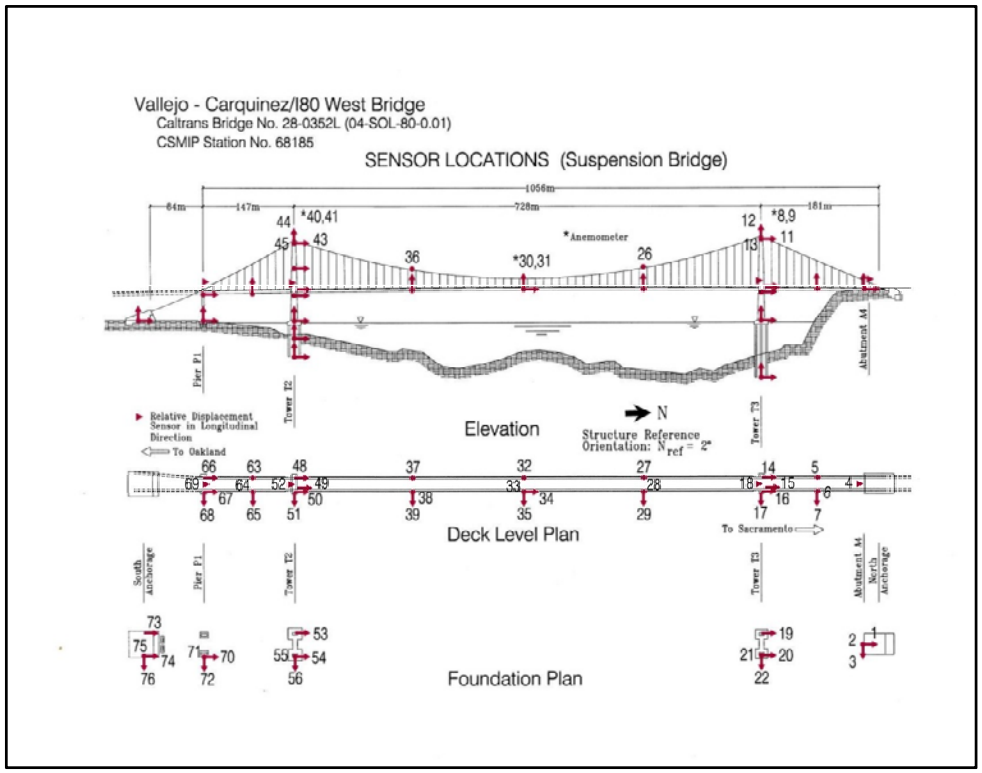

Figure 11. Foundation Plan with Sensor Locations

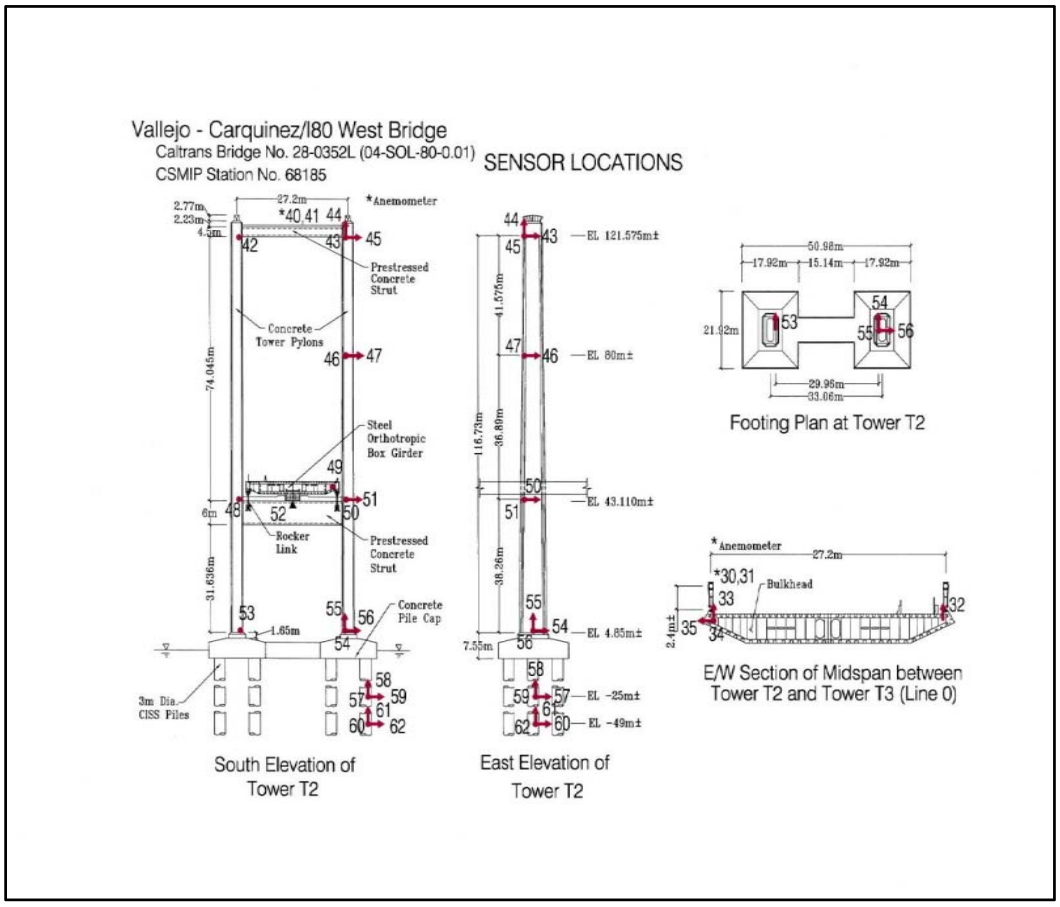

Figure 12. Substructure Components Showing Locations for the Development of Fragility Functions

Based on this work Vosooghi and Saiidi (2012) proposed five distinct apparent damage states (DSs) for reinforced concrete columns subjected to earthquakes, as follows:

- DS-1: Flexural cracks;
- DS-2: Minor spalling and possible shear cracks;
- DS-3: Extensive cracks and spalling;
- DS-4: Visible lateral and/or longitudinal cracks and/or visible reinforcing bars;
- DS-5: Compressive failure of the concrete core edge (i.e., imminent failure).

It is envisioned that both the analytical and recorded test data along with the photographed damage will be key in developing the fragility data that can be related to operability of the bridge and aid in the decision to keep the bridge open for public and/or emergency vehicles, or to close the bridge to all traffic.

Nonlinear quasi-static (push-over) Analysis

Push-over analysis will be conducted on Tower 3 using the ADINA model for the as-built plans and materials using the response spectrum for the design hazard to determine actual capacity of the tower and to determine if the intensity of the applied ground motion is below or above the design earthquake.

References

Abrahamson, N.A. (2000) "Effects of rupture directivity on probabilistic seismic hazard analysis", Proceedings of the Sixth International Conference on Seismic Zonation, Earthquake Engineering Research Inst., Oakland, California.

Abrahamson, N.A., W. J. Silva, and R. Kamai, (2014) "Summary of the ASK14 Ground Motion Relation for Active Crustal Regions." Earthquake Spectra: August 2014, Vol. 30, No. 3, pp. 1025-1055.

ADINA Toll Bridges Project, sponsored by California Department of Transportation, Caltrans, 2014.

ADINA R&D, Theory and Modeling Guide, Vol. I. Watertown, MA: ADINA Solids & Structures, 2009.

American Society of Civil Engineers (1998). "Seismic Analysis of Safety-Related Nuclear Structures and Commentary." Reston, VA: ASCE, 19998. 978-0-7844-0433-1.

American Society of Civil Engineers (2005). "Seismic Design Criteria for Structures, Systems, and Components in Nuclear Facilities." American Society of Civil Engineers, 2005. ASCE/SEI 43-05.

Ancheta, T.D., Robert B. Darragh, Jonathan P. Stewart, Emel Seyhan, Walter J. Silva, Brian S.-J. Chiou, Katie E. Wooddell, Robert W. Graves, Albert R. Kottke, David M. Boore, Tadahiro Kishida, and Jennifer L. Donahue (2014) "NGA-West2 Database." Earthquake Spectra: August 2014, Vol. 30, No. 3, pp. 989-1005.

Atik, L.A. and Abrahamson, N. (2009) "An Improved Method for Nonstationary Spectral Matching." Earthquake Spectra, Vol. 26, No. 3, pp 601-617.

Baker, J.W. (2011). "Conditional Mean Spectrum: Tool for ground motion selection," Journal of Structural Engineering, Vol. 137 No.3, pp 322-331.

Boore, D. M., J. P., Stewart, E. Seyhan, and G.G., Atkinson. (2014) "NGA-West2 Equations for Predicting PGA, PGV, and 5% Damped PSA for Shallow Crustal Earthquake." Earthquake Spectra: August 2014, Vol. 30, No. 3, pp. 1057-1085.

Caltrans (2010), Data DVD provided by Steve Mitchell of Caltrans to Hassan Sedarat of SC Solutions on December 13, 2010.

Caltrans, Construction Marked up Drawings of Alfred Zampa Memorial Bridge.

Caltrans Contract 59A007, "3rd Carquinez Strait Bridge Seismic Report"

Caltrans Contract No. 59A007, "Third Carquinez Strait Bridge Structural Design Criteria"

Campbell, K.W. and Bozorgnia, Y., (2014) "NGA-West2 Ground Motion Model for the Average Horizontal Components of PGA, PGV, and 5% Damped Linear Acceleration Response Spectra." Earthquake Spectra 30:3, 1087-1115.

Chiou, B.S.J. and Young, R. R., (2014) "Update of the Chiou and Youngs NGA Model for the Average Horizontal Component of Peak Ground Motion and Response Spectra." Earthquake Spectra: August 2014, Vol. 30, No. 3, pp. 1117-1153.

De Leuw–OPAC–Steinman (DLOS) (1999) "Third Carquinez Strait Bridge, Seismic Report, 100% submittal", San Francisco, CA, February 1999

EMI (2014) "Kinematic Soil Pile Interaction for New Carquinez Bridge." Technical Memorandum, March 24, 2014, Earth Mechanics, Inc., Fountain Valley, CA

Gülerce, Z. and Abrahamson, N.A. (2011) "Site-Specific Design Spectra for Vertical Ground Motion." Earthquake Spectra: November 2011, Vol. 27, No. 4, pp. 1023-1047.

Hassan Sedarat, Iman Talebinejad, Abbas Emami-Naeini, David Falck, Gwendolyn van der Linden, Farid Nobari, Alex Krimotat, Jerome Lynch (2014), "Real-Time Estimation of the Structural Response using Limited Measured Data", SPIE Smart Structures and Materials + Nondestructive Evaluation and Health Monitoring, Nondestructive Characterization for Composite Materials, Aerospace Engineering, Civil Infrastructure, and Homeland Security 2014, Proceeding of SPIE Vol. 9063, 906311 © 2014 SPIE.

Hassan Sedarat, Alexander Kozak, Joyce Lee, Alex Krimotat, Vince Jacob, and Steve Mitchell (2013), "Efficient Techniques in Finite Element Analysis and Seismic Evaluation of Suspension Bridges", , 7NSC, Seventh National Seismic Conference on Bridges & Highways, Oakland, CA, May 20-22, 2013.

Hassan Sedarat, SC-Cable, Suspension Bridge Construction Sequence Application, SC Solutions, Inc., Sunnyvale, CA.

Jayaram, N., and Baker, J. W., (2008) "Statistical Tests of the Joint Distribution of Spectral Acceleration Values" Bulletin of the Seismological Society of America, Vol. 98, No. 5, pp. 2231-2243,

Kurata, M., Kim, J., Lynch, J.P., van der Linden, G., Sedarat, H., Thometz, E., Hipley, P. and Sheng, L.H., "Inter- net-Enabled Wireless Structural Monitoring Systems: Development and Permanent Deployment at the New Carquinez Suspension Bridge", ASCE Journal of Structural Engineering

OPAC Calculation Book Volume 4 – Seismic Analysis Calculation.

SCS (2015) "Rapid Post-Earthquake Safety Evaluation of the New Carquinez Bridge Using Fragility Curves and Strong-Motion Data: Seismic Hazard Memorandum." March 18, 2015, SC Solutions, Inc., Sunnyvale CA

Shahi, S.K. and Baker, J. W. (2011) "An Empirically Calibrated Framework for Including the Effects of Near-Fault Directivity in Probabilistic Seismic Hazard Analysis." Bulletin of the Seismological Society of America, Vol. 101, No. 2, pp. 742–755

Sleeter, B.B., Calzia, J.P., Walter, S. R., Wong, F.L., and Saucedo G. J., (2004), "Earthquakes and faults in the San Francisco Bay Area (1970-2003)" http://pubs.usgs.gov/sim/2004/2848/, Last access, 085/27/2015;

Vosooghi, Ashkan and Saiidi, M. Saiid (2010), "Seismic Damage States and Response Parameters for Bridge Columns" ACI Special Publication Series SP-271, Structural Concrete in Performance –Based Seismic Design of Bridges, 271 CD, 2010

Vosooghi, Ashkan and Saiidi, M. Saiid (2012), Experimental Fragility Curves for Seismic Response of Reinforces Concrete Bridge Columns" ACI Structural Journal, November/December, 2012 pp 825-834